Biochimica et Biophysica Acta 1822 (2012) 301–313

Contents lists available at SciVerse ScienceDirect

Biochimica et Biophysica Acta

journal homepage: www.elsevier.com/locate/bbadis

Up-regulation of NDRG2 through nuclear factor-kappa B is required for Leydig cell apoptosis in both human and murine infertile testes

Teng Li [a,1], Jing Hu [a,1], Gong-Hao He [b,1], Yun Li [a], Chu-Chao Zhu [a], Wu-Gang Hou [a], Shun Zhang [a], Wei Li [a], Jin-Shan Zhang [a], Zhe Wang [c], Xin-Ping Liu [d], Li-Bo Yao [d,*], Yuan-Qiang Zhang [a,*]

[a] Department of Human Anatomy, Histology and Embryology, The Fourth Military Medical University, Xi'an 710032, China
[b] Department of Pharmacy, Kunming General Hospital of Chengdu Military Region, Kunming 650032, China
[c] Department of Pathology, The Fourth Military Medical University, Xi'an 710032, China
[d] Department of Biochemistry and Molecular Biology, The State Key Laboratory of Cancer Biology, The Fourth Military Medical University, Xi'an 710032, China

ARTICLE INFO

Article history:
Received 30 July 2011
Received in revised form 4 November 2011
Accepted 14 November 2011
Available online 22 November 2011

Keywords:
Nuclear factor-kappa B
N-*myc* downstream-regulated gene 2
Infertile disease
Leydig cell
Apoptosis
Pyrrolidine dithiocarbamate

ABSTRACT

Many pro-apoptotic factors, such as nuclear factor-kappa B (NF-κB) and Fas, play crucial roles in the process of Leydig cell apoptosis, ultimately leading to male sterility, such as in Sertoli cell only syndrome (SCO) and hypospermatogenesis. However, the molecular mechanism of such apoptosis is unclear. Recent reports on N-*myc* downstream-regulated gene 2 (*ndrg2*) have suggested that it is involved in cellular differentiation, development, and apoptosis. The unique expression of NDRG2 in SCO and hypospermatogenic testis suggests its pivotal role in those diseases. In this study, we analyzed NDRG2 expression profiles in the testes of normal spermatogenesis patients, hypospermatogenesis patients, and SCO patients, as well as *in vivo* and *in vitro* models, which were Sprague–Dawley rats and the Leydig cell line TM3 treated with the Leydig cell-specific toxicant ethane-dimethanesulfonate (EDS). Our data confirm that NDRG2 is normally exclusively located in the cytoplasm of Leydig cells and is up-regulated and translocates into the nucleus under apoptotic stimulations in human and murine testis. Meanwhile, transcription factor NF-κB was activated by EDS administration, bound to the *ndrg2* promoter, and further increased in expression, effects that were abolished by NF-κB inhibitor Pyrrolidine dithiocarbamate (PDTC). Furthermore, siRNA knock-down of *ndrg2* led to increased proliferative or decreased apoptotic TM3 cells, while over-expression of *ndrg2* had the reverse effect. This study reveals that *ndrg2* is a novel gene that participates in Leydig cell apoptosis, with essential functions in testicular cells, and suggests its possible role in apoptotic Leydig cells and male fertility.

1. Introduction

Spermatogenesis is a dynamic process that requires the cooperation of distinct compartments of the testis, seminiferous tubules, and the interstitial tissues [1]. Leydig cells constitute the majority of interstitial cells and generate testosterone for spermatogenesis [1]. Leydig cell abnormality is prevalent in infertile diseases. Hyperplasia of Leydig cell was observed in transgenic mouse over-expresses human chorionic gonadotropin [2], while Leydig cell apoptosis was found in the testes of maturation arrest (MA) and SCO patients [3]. Furthermore, such apoptosis often accompanied with massive germ cell apoptosis, mostly due to abnormal hormone level. Thus, elucidating the mechanism of Leydig cell apoptosis would help us to understand and treat those diseases. Leydig cell apoptosis could be triggered by many factors, including exposure to radiation, toxic substances, hypoxia, ischemia and stress [4–7]. To clarify the possible mechanism of Leydig cell apoptosis both *in vivo* and *in vitro*, EDS has been used to stimulate Leydig cell apoptosis [8]. Both the apoptosis of Leydig cells triggered by EDS and decreased spermatogenesis are irrelevant in the apoptotic pathway involving the *bcl-2* gene family and p53 [9] but should be accounted for in the Fas/Fas-L and caspase-3 system activation [3,10,11].

In this study, a novel gene, *ndrg2*, was investigated in Leydig cell apoptosis due to its exclusive expression in Leydig cells among all testicular cells [12,13]. It was identified in a human brain cDNA library by PCR-based subtractive hybridization in 1999, and is a member of the differentiation-related NDRG family, which includes four members, NDRG1, -2, -3, and -4 [14]. NDRG2 is expressed in brain, heart,

Abbreviations: B2M, beta-2-microglobulin; ChIP, chromatin immunoprecipitation; DAB, diaminobenzidine; EDS, ethane-dimethanesulfonate; EdU, 5-ethynyl-2′-deoxyuridine; FBS, fetal bovine serum; gapdh, glyceraldehyde-3-phosphate dehydrogenase; hprt1, hypoxanthine phosphoribosyl-transferase 1; 3β-HSD, 3β-hydroxysteroid dehydrogenase; 17β-HSD, 17β-hydroxysteroid dehydrogenase; MA, maturation arrest; MAA, methoxyacetic acid; ndrg2, N-myc downstream-regulated gene 2; NF-κB, nuclear factor-kappa B; PDTC, pyrrolidine dithiocarbamate; RIP-1, regulated intramembrane proteolysis-1; TNF-α, tumor necrosis factor-alpha; PI, propidium iodide; TUNEL, terminal deoxynucleotidyl transferase dUTP nick end labeling; SCO, Sertoli cell only syndrome.

* Corresponding author.
E-mail addresses: bioyao@fmmu.edu.cn (L.-B. Yao), zhangyq@fmmu.edu.cn (Y.-Q. Zhang).

[1] These authors contributed equally to this paper.

0925-4439/$ – see front matter © 2011 Elsevier B.V. All rights reserved.
doi:10.1016/j.bbadis.2011.11.013

skeletal muscle, and many other tissues [13]. It might be involved in the suppression of tumor cell proliferation due to its decreased expression in several types of tumors [15–20]. In the human lung cancer cell line A549, *ndrg2* is regulated by hypoxia-inducible factor 1 [21]. Its modulation by p53 in several tumor cell lines suggests that *ndrg2* might participate in the apoptotic process [22]. More importantly, NDRG2 has been correlated with Fas expression and Fas-mediated cell death in gastric cancer cells [23]. Additionally, in two metastatic tumor cell lines, inhibition of NDRG2 affects the activation of NF-κB [24], a classical apoptotic factor and Fas downstream molecular [25]. NF-κB is also involved in Leydig cell apoptosis induced by glucocorticoid [26]. However, the connection between NF-κB and NDRG2 in Leydig cells remains unclear. Thus, elucidating their regulation and potential interaction, as a putative mechanism of Leydig cell apoptosis, might shed light on male sterility.

2. Materials and methods

2.1. Testicular samples

Testicular specimens were obtained from 25 men with a normal 46, XY karyotype and with obstructive or nonobstructive azoospermia who visited the male infertility clinic in Xi Jing Hospital (Xi'an, China): 17 men with nonobstructive azoospermia and from 8 men with obstructive azoospermia. The open testicular biopsy technique was used to obtain these specimens. Informed consent was obtained from all patients. Tissues were fixed in Bouin's solution prior to processing for paraffin embedding.

On the basis of standard qualitative interpretations of hematoxylin and eosin-stained sections (Fig. 1A), biopsies were classified as follows: normal (NOR; n = 8), almost all tubules showed development of more than 10 elongating spermatids in each tubule cross section; hypospermatogenesis (n = 6), all tubules showed deranged spermatogenesis; congenital SCO (n = 6), all seminiferous tubules showed deletion of germ cells in the epithelium, while Leydig cell appears to be normal in number and shape; secondary SCO (n = 5), the diameter of the tubules is variable, ranging from normal to very tiny ones, and the Sertoli cells are diminished in number and highly altered in shape, only a few Leydig cells can be seen around the tubules [27]. The testicular specimens from obstructive azoospermia showing normal spermatogenesis (NOR) were used as a control. For detailed information of patients' serum testosterone level, see Table 1.

2.2. Plasmid and siRNA constructions

DNA fragments encoding NF-κB binding sites in the mouse *ndrg2* promoter (−1943 bp to +249 bp) were amplified by PCR, using LA *Taq* enzyme (Takara, Tokyo, Japan) and the mouse genome as template with the following primers: F 5′-GC AGA TCT ATG AGG CAG AGG CAG TTT-3′ and R 5′-GC AAG CTT ACA GCC AGG AGA CCA GAA-3′. These fragments were cloned into the pGL3-*luc* vector (Promega, MD, USA) with Bgl II and Hind III. The truncated vector was generated either by Kpn I digestion (−1943 bp to −210 bp) or by PCR using mouse *ndrg*2 promoter-pGL3-*luc* vector as template with following primers: (−1463 bp to +249 bp) F 5′-GC AGA TCT GAG AAA A GA ACA GAG GGA A AC-3′, R 5′-GC AAG CTT ACA GCC AGG AGA CCA GAA-3′; (−995 bp to +249 bp) F 5′-GC AGA TCT CAG TCC ATC AAC

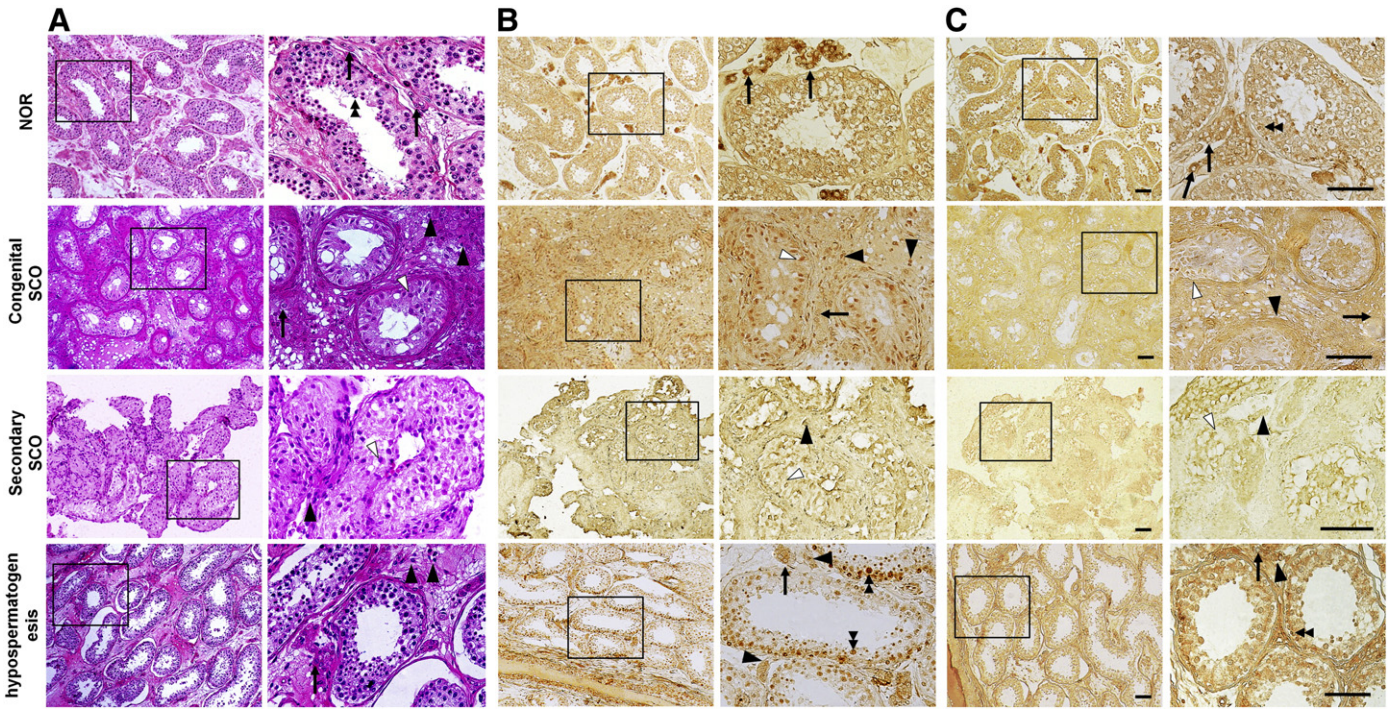

Fig. 1. Histological analysis of NDRG2 and NF-κB in normal, congenital SCO, secondary SCO and hypospermatogenic testes. (A) HE staining of normal, congenital SCO, secondary SCO and hypospermatogenic testes. In testes with normal spermatogenesis, cells in the seminiferous tubules were well arranged, and elongated spermatids were seen. In testes of both congenital and secondary SCO patients, all tubules contained only Sertoli cells. In hypospermatogenic testes, the number of each stage of germ cells decreased, and the spermatogenic epithelium was thinner. Arrows: healthy Leydig cells; solid arrowheads: apoptosis-like Leydig cells; open arrowheads: Sertoli cells; dual arrowheads: elongated spermatids. (B) Immunohistochemistry for NDRG2 in normal and aberrant testes. Intensive staining for NDRG2 was found in the cytoplasm of the healthy Leydig cells, whereas in congenital SCO, secondary SCO and hypospermatogenic testes, the signal for NDRG2 was located in the nuclei of Leydig cells, Sertoli cells and germ cells. Arrows: Leydig cells with NDRG2 staining in cytoplasm; solid arrowheads: Leydig cells with NDRG2 staining in the nuclei; open arrowheads: Sertoli cells with NDRG2 staining in the nuclei; dual arrowheads: germ cells with NDRG2 staining in the nuclei. (C) Characterization of NF-κB expression in normal and aberrant testes. Relatively intense staining for NF-κB was found in the cytoplasm of the healthy Leydig cells and nuclei of spermatogonia, whereas in two types of SCO and hypospermatogenic testes, the signal for NF-κB was located in the nuclei of Leydig cells, Sertoli cells and germ cells. Both sections show two images at lower and higher magnification, respectively. Arrows: Leydig cells with NF-κB staining in cytoplasm; solid arrowheads: Leydig cells with NF-κB staining in the nuclei; open arrowheads: Sertoli cells with NF-κB staining in the nuclei; dual arrowheads: germ cells with NF-κB staining in the nuclei. Data represent groups of patients (normal, n = 8; congenital SCO, n = 6; secondary SCO, n = 5; hypospermatogenesis, n = 6) (scale bars 50 μm).

Table 1
Analysis of NDRG2, NF-κB, TUNEL positive signals in Leydig cell nucleus and serum testosterone level from men with different histological diagnosis.

Diagnosis	NDRG2 (%labeled cells)	NF-κB (%labeled cells)	TUNEL (%labeled cells)	Serum T (ng/ml)
Normal spermatogenesis	0.24 ± 0.12	1.35 ± 0.72	0.19 ± 0.07	8.47 ± 1.14
Congenital SCO	37.95 ± 7.58*	34.22 ± 8.24*	39.47 ± 9.36*	7.38 ± 1.72
Secondary SCO	89.82 ± 3.03*	92.35 ± 2.59*	95.86 ± 6.18*	5.53 ± 0.57*
Hypospermatogenesis	22.83 ± 5.27*	19.40 ± 3.21*	15.19 ± 7.13*	8.26 ± 2.31

Note: Data are presented as mean ± SEM. Three hundred cells were evaluated for each patient. *Significantly different from group of normal spermatogenesis. $P<0.05$.

CGT TCC-3′, R 5′-GC AAG CTT ACA GCC AGG AGA CCA GAA-3′; (−449 bp to +249 bp) F 5′-GC AGA TCT GAC TCG GCT GAG GAG GTA-3′, R 5′-GC AAG CTT ACA GCC AGG AGA CCA GAA-3′. The phRL-CMV plasmid (Promega), which contains a Renilla luciferase gene under the control of a constitutive SV40 promoter, served as the control vector. The *ndrg2*-pcDNA3.1 plasmid and was kindly provided by Prof. Xinping Liu (Fourth Military Medical University, Xi'an, China). All plasmids were verified by sequencing (AuGCT, Beijing, China). The sequences of siRNAs (Gene-Pharma, Shanghai, China) used were: mouse *ndrg2* sense: U CAA CAG GAG ACU UCC AUG GUG UGC; antisense: G CAC ACC AUG GAA GUC UCC UGU UGA; non-silencing control (labeled with FAM) sense: UUC UCC GAA CGU GUC ACG UTT; antisense: ACG UGA CAC GUU CGG AGA ATT; *gapdh* sense: GUA UGA CAA CAG CCU CAA GTT; antisense: CUU GAG GCU GUU GUC AUA CTT.

2.3. Animals and reagents

Sprague–Dawley male rats (90 days old) and c57BL/6J male mice (60 days old) (Fourth Military Medical University, Xi'an, China) were injected intraperitoneally with either a single dose of EDS (75 mg/kg for rat as described previously [8]; 75 mg/kg, 150 mg/kg, or 375 mg/kg for mouse), or with vehicle. PDTC (100 mg/kg body weight) [28] was injected into rat abdominal cavity immediately after EDS treatment. EDS was produced in our lab according to the Jackson Lab protocol [29] in a vehicle of DMSO/H_2O (1:3 v/v). Animals were euthanized at 2 h, 6 h, 12 h, 24 h, 48 h, or 72 h (mouse groups and PDTC groups only at 72 h) after treatment. One of the testes was prepared for histologic examination; the other testis was immediately frozen in liquid nitrogen until analysis. The Ethics Committee for Animal Experiments of the Fourth Military Medical University approved all animal work and experimental protocols.

Reagents used in this study and their vendors are as follows: LA *Taq* enzyme, PrimeScript RT reagent kit, SYBR Premix EX *Taq* II (Takara); Bgl II, Kpn I and Hind III, Dual-Luciferase Reporter Assay System (Promega); *In Situ* Cell Death Detection Kit, POD (Roche, PA, USA); fetal bovine serum (FBS), horse serum, Lipofectamine 2000, TRIzol reagent (Invitrogen, CA, USA); DMEM-F12, NE-PER nuclear and cytoplasmic extraction reagents (Thermo, MA, USA); hematoxylin and eosin-Y, PDTC, diaminobenzidine (DAB), DMSO (Sigma-Aldrich, Shanghai, China); tumor necrosis factor-alpha (TNF-α, provided by Prof. Yingqi Zhang, Fourth Military Medical University, Xi'an, China); fluorescein isothiocyanate (FITC)-labeled Annexin V and propidium iodide (PI) (Bestbio, Shanghai, China); Cell-Light™ thymidine nucleotide analogue 5-ethynyl-2′-deoxyuridine (EdU) staining kit (Ribobio, Guangzhou, China). Antibodies used are listed in Table 2.

2.4. Purification of Leydig cells

Rat Leydig cells were purified from the vehicle-, EDS- and/or PDTC-treated testes by continual Percoll density-gradient centrifugation, as described in our previous study [29]. The purity of isolated Leydig cells was characterized by staining with anti-3β-hydroxysteroid dehydrogenase (3β-HSD) antibody (see Table 2). The purified Leydig cells (purity > 92%) were used for the following experiments.

Table 2
Antibodies, vendors, applications and their working dilutions.

Antibody	Vendor	Application	Working dilution
Mouse anti-NDRG2 monoclonal antibody	Abnova, Taiwan	IHC, IF WB	1:100 1:300
Mouse ExtrAvidin Peroxidase Staining Kit	Sigma-Aldrich, USA	IHC	1:20
Rabbit anti-3β-HSD polyclonal antibody	Santa Cruz biotechnology Inc, USA	IF	1:100
Tritc-conjugated goat anti-mouse IgG	Sigma-Aldrich, USA	IF	1:60
Cy5-conjugated donkey anti-rabbit IgG	Chemicon, Millipore, USA	IF	1:200
Mouse anti-NF-κB p65 monocolonal antibody	Santa Cruz biotechnology Inc, USA	IHC, IF WB	1:100 1:500
FITC-conjugated goat anti-mouse IgG	Sigma-Aldrich, USA	IF	1:60
Mouse anti-Fas intracellular fragment monoclonal antibody	Abcam, USA	WB	1:200
Rabbit anti-caspase 3 polyclonal antibody	Abcam, USA	WB	1:300
Rabbit anti-active-caspase-3 p17 polyclonal antibody	Bioworlde, USA	WB	1:300
Mouse anti-α-tubulin (TU-16) monocolonal antibody	Santa Cruz biotechnology Inc, USA	WB	1:1000
Rabbit anti-Histone H2A.X (Ab-139) polyclonal antibody	Signalway Antibody, USA	WB	1:300
IRDye 800 CW conjugated goat anti-mouse IgG	Rockland Inc, IL, USA	WB	1:15,000
IRDye 800 CW conjugated goat anti-rabbit IgG	Rockland Inc, IL, USA	WB	1:15,000

Antibodies used for various experiments as reported herein are listed. Note that these antibodies cross-reacted with the corresponding rat and/or mouse proteins as noted by the manufacturers if the source of antigens used to raise the antibodies was not from rats or mouse. WB, Western blot; IHC, immunohistochemistry; IF, immunofluorescence.

2.5. Cell culture and transfection

The mouse Leydig cell line TM3 (American Tissue Culture Collection) was cultured in DMEM-F12, 2.5% FBS and 5% horse serum at 37 °C in a 5% CO_2 atmosphere.

At 24–48 h after purification, 2×10^5/ml cells were seeded into 6-well plates and incubated with culture medium containing vehicle, 200 μmol PDTC and/or 1.0 mg/ml EDS, according to previous reports [30,31]. For PCR and western blot, cells were lysed after 2 h, 6 h, 12 h, and 24 h, collected for RNA and protein extraction, and stored at −80 °C.

All siRNAs and plasmids were transfected into cells with Lipofectamine 2000. Transfection with the non-silencing control 5′-FAM-labeled siRNA and a green fluorescent protein (GFP)-pcDNA3.1 plasmid demonstrated that 80%–90% and 60%–70%, respectively, of the cells were transfected, as detected by fluorescence microscopy (Olympus IX71S8F-2, Tokyo, Japan) (Supplementary Fig. 1A, B, C and D).

2.6. HE and immunohistochemistry

Paraffin sections of the testes were stained with hematoxylin for 3 min, followed by 1 min incubation with Clarifier I and Bluing Reagent, and then stained with eosin-Y for another 30 s. Apoptotic Leydig cells were determined by morphology characteristics, such as lack

of cell contact, condensation of chromatin near the nuclear membrane, shrinkage of cell volume and formation of apoptotic bodies. Relative Leydig cell number was obtained through amplification *17β-HSD* III (for primers, see Section 2.9), marker of the adult Leydig cell [32].

For immunohistochemistry, the sections were blocked with 10% normal goat serum for 1 h and probed with anti-NDRG2 antibody or anti-NF-κB antibody at 4 °C overnight. Then they were incubated with biotinylated goat anti-mouse IgG at room temperature for 2 h and incubated with ExtrAvidin Peroxidase for 1 h. Positive staining was detected with 0.05% DAB/0.01% H_2O_2 in 0.05 mol/l Tris–HCl buffer. The EDS-treated rat testicular sections of NDRG2 were then counterstained with hematoxylin for 2 min, while this step was omitted for NF-κB sections. The negative control group, in which one of the primary antibodies was omitted and replaced with normal IgG, showed no immunoreactivity (Supplementary Fig. 2A). All photographs were taken under a light microscope (ZEISS Imager M1, Germany).

2.7. Terminal deoxynucleotidyl transferase dUTP nick end labeling (TUNEL) and immunofluorescent analysis of the apoptotic Leydig cells

The expression of NDRG2 and 3β-HSD in apoptotic Leydig cells post-EDS treatment both *in vivo* and *in vitro* was assessed by immunofluorescence combined with TUNEL assay. TUNEL staining to identify apoptotic Leydig cell *in situ* was performed as instructed by the *In Situ* Cell Death Detection Kit. After incubation with TUNEL reaction mixture, those sections were labeled with the mixture of anti-NDRG2 antibody and anti-3β-HSD antibody (see Table 2) at 4 °C overnight. TRITC- or Cy5-conjugated secondary antibodies (see Table 2) were mixed and added onto the sections for 2 h and then cover-slipped. Two negative controls and a positive control were set up according to the manufacturer's protocol (Supplementary Fig. 2B, C).

The spatial expression of NF-κB and NDRG2 after EDS and TNF-α treatment was evaluated with immunofluorescence using anti-NDRG2 antibody or anti-NF-κB p65 antibody (see Table 2) at 4 °C overnight. Then the slides were labeled with TRITC- or FITC-conjugated goat anti mouse IgG (see Table 2) at room temperature for 2 h and cover-slipped. The specificity of the antibody was controlled by using normal IgG instead of the primary antibody (Supplementary Fig. 2D).

All labeled sections were observed under a confocal laser-scanning microscope (Olympus FV1000) with excitation at 488 nm for FITC/apoptotic cells or NF-κB p65, 543 nm for TRITC/NDRG2 and 650 nm for Cy5/3β-HSD.

2.8. Protein extraction and western blot analysis

The lysates of collected tissues and cells were prepared in lysis buffer containing 150 mM NaCl, 2 mM EGTA, 10% glycerol (v/v), and 1% Nonidet P-40 (v/v) at pH 7.4 under 22 °C. Samples were freshly supplemented with a 100:1 (v/v) ratio of protease inhibitor cocktail to phosphatase inhibitor cocktails 1 and 2. Proteins (40 μg) were separated by SDS-PAGE and transferred onto nitrocellulose membranes. Membranes were saturated with Tris-buffered saline with 0.1% Tween 20 and 3% bovine serum albumin (TBST-BSA) and were probed with the appropriate antibodies (see Table 2). Equal protein loading for tissue or whole-cell lysates was assessed by stripping blots and reprobing with an anti-tubulin antibody or anti-histone antibody (see Table 2) for nuclear extracts. Secondary antibodies conjugated to IRDye 800 CW were detected by an Odyssey infrared imaging system (LI-COR Inc, Lincoln, NE).

2.9. RNA extraction and quantitative real-time PCR analysis

Total RNA was extracted from the testis specimens and TM3 cells using TRIzol reagent according to the manufacturer's instructions. Those RNAs were reverse-transcribed to cDNAs according to Takara's reverse transcription system protocol. cDNAs were then amplified by PCR using specific primers for mouse *ndrg2* and *17β-HSD* III: *ndrg2* F 5′-T CGT GCG GGT TCA TGT GGA TGC-3′, R 5′-T GTG TCC GGG TGG TTC AGA GCA-3′, product size 203 bp; *17β-HSD* III F 5′-ATT TTA CCA GAG AAG ACA TCT-3′, R 5′-GGG GTC AGC ACC TGA ATA ATG-3′, product size 367 bp. The primer sequences for *hprt1*, *B2M*, *gapdh*, which was used as internal quantitative controls for the amplification, were as follows: *hprt1* F 5′-AGC TAC TGT AAT GAT CAG TCA ACG-3′, R 5′-AG AGG TCC TTT TCA CCA GCA-3′, product size 198 bp; *B2M* F 5′- C ATG GCT CGC TCG GTG ACC-3′, R 5′-AAT GTG AGG CGG GTG GAA CTG-3′ product size 166 bp; *gapdh* F 5′-CC AGG TTG TCT CCT GCG ACT TCA-3′, R 5′-GGG TGG TCC AGG GTT TCT TAC TCC-3′, product size 189 bp. The PCR enzyme and reagents used were SYBR Premix EX *Taq* II. Cycling conditions for *ndrg2*, *hprt1*, *B2M*, and *gapdh* were 95 °C for 30 s, followed by 40 cycles of 95 °C for 3 s and 60 °C for 30 s (ABI PRISM 7500 Real-Time PCR System, Life Technologies, USA). The quantitative PCR was run in singleplex in triplicate for each sample. Data were analyzed using the ABI Prism 7500 SDS software and genorm^{plus} software (Biogazelle NV, Zwijnaarde, Belgium) as previously described [33,34].

2.10. Quantification of apoptosis

Apoptosis was quantified by flow cytometry analysis. Briefly, 2×10^5/ml TM3 cells were cultured in 6-well plates with medium containing vehicle, PDTC (200 μmol) and/or EDS (1.0 mg/ml) for 2 h, 6 h, 12 h, or 24 h. Cells were collected by trypsinization and washed with PBS. Apoptosis was measured by dual-color analysis of Annexin V binding (green fluorescence) and PI uptake (red fluorescence) using a FACSCalibur (Becton Dickinson, CA, USA) apparatus with excitation and emission settings at 488 nm plus a 515 nm band pass filter for fluorescein detection and a filter at >600 nm for PI detection.

2.11. Luciferase reporter gene assay

A total of 10^4 cells/well of TM3 cells were seeded into 96-well plates and were cultured for 24 h before transfection. Then 0.4 μg/well pGL3-mouse *ndrg2* promoter-*luc* plasmid or a pGL3-truncated mouse *ndrg2* promoter-*luc* plasmid was co-transfected with 0.1 μg/well phRL-CMV plasmid into TM3 cells with 0.5 μl/well Lipofectamine 2000. Forty-eight hours later, cells were incubated with either TNF-α (100 ng/ml), EDS (1.0 mg/ml), PDTC (200 μmol) or vehicle for 8 h. Subsequently, cells were lysed, and activation of the pGL3-mouse *ndrg2* promoter-*luc* construct was measured using the Dual-Luciferase Reporter Assay System according to the manufacturer's instructions. Luminescence was quantified using a GLOMAX™ 20/20 luminometer (Promega). Three independent experiments were done at least in quadruplicate, and the luciferase values were normalized to Renilla luminescence.

2.12. Preparation of cytoplasmic and nuclear extracts

The cytoplasmic and nuclear protein extracts were prepared with the NE-PER nuclear and cytoplasmic extraction reagents according to the manufacturer's instructions. Samples were stored at −80 °C for western blot analysis.

2.13. Labeling and detecting the DNA of proliferating cells with 5-ethynyl-2′-deoxyuridine (EdU) in vitro

The Cell-Light ™ EdU staining kit was used for the *in vitro* labeling of the nuclei of dividing cells. Negative controls with EdU incubation omitted showed no positive signal (Supplementary Fig. 2E, F). Images were acquired under a fluorescence microscope (ZEISS Imager M1).

2.14. Chromatin immunoprecipitation (ChIP)

ChIP assays were performed with the chromatin immunoprecipitation assay kit (Millipore, Upstate, Temecula, CA) according to the manufacturer's instructions. Briefly, TM3 cells were seeded in 10-cm culture dishes. After treatment with TNF-α (100 ng/ml), EDS (1.0 mg/ml), PDTC (200 μmol) or vehicle for 2 h, cells were cross-linked with 1% formaldehyde for 15 min and sonicated at 100 W followed by centrifugation for 15 min at 13,000×*g* at 4 °C. Supernatant (40 μl) was taken as an input control, and the rest of the sample was pre-cleaned with 75 μl agarose/salmon sperm and divided into four portions. Two micrograms of immunoprecipitating antibody against NF-κB (see Table 2) and normal rabbit IgG was added to each portion. After overnight incubation at 4 °C, antibody–histone–DNA complexes were sequentially washed with low-salt buffer, high-salt buffer, LiCl immune buffer, and TE buffer. Precipitates were eluted and incubated at 65 °C overnight to reverse formaldehyde cross-linking by adding 20 μl 5 M NaCl. DNA was purified by phenol/chloroform extraction and ethanol precipitation. The chromatin fragments were amplified by PCR using primers flanking the NF-κB binding sites of the *ndrg2* promoter as follows: (−1856 to −1735) F 5′-A GGT CTA GGA AGT AAA CAG ATC-3′, R 5′-A GGT TCC AGC ATC TAA ATC-3′, product size 122 bp; (−1340 to −1161) F 5′-CTC CTC CTC CTC CCT CTT-3′, R 5′-CTG CCA ACT GCA ACA CCA-3′, product size 180 bp; (−702 to −557) F 5′-CCA CCC TTG CAG AGT TAG-3′, R 5′-GAA GGA GGG GAA AGA TGA-3′, product size 146 bp; (−463 to −352) F 5′-AGA GCA AGC GGC GGG ACT-3′, R 5′-CTC GGG GCA GGT ATG GGT-3′, product size 117 bp.

2.15. Statistical analysis

One-way ANOVA followed by Scheffe's *F* test (for multiple comparisons) or two-way ANOVA (for entire curves) was performed to compare the effects of treatments on experiments with >2 treatment groups. Student's *t* test was used to compare 2 group-design experiments. Statistical analyses were performed with SPSS software (version 10.0; SPSS, Chicago, IL). Results are presented as mean ± SEM from at least three independent experiments unless otherwise stated. Statistical significance was defined as $P<0.05$.

3. Results

3.1. Expression of NDRG2 and NF-κB in normal and infertile human testes

HE staining of normal and infertile testes served as standards of diagnosis (Fig. 1A). In the case of normal spermatogenesis, NDRG2 expression was detected in the cytoplasm of interstitial Leydig cells (Fig. 1B). In hypospermatogenic testes, intensive NDRG2 immunostaining was observed in the nuclei of Leydig cells and degenerating germ cells (Fig. 1B), while NDRG2 expression was strongly detected

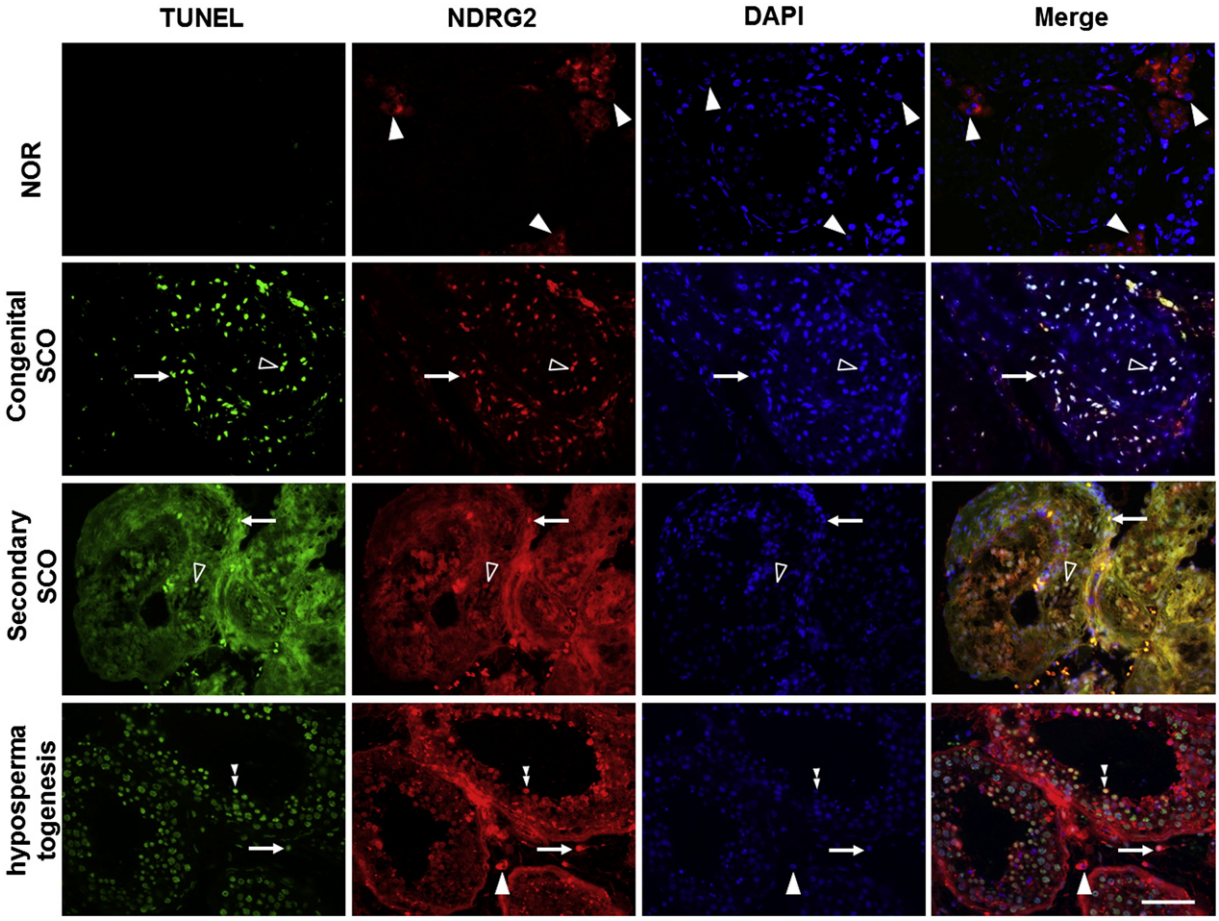

Fig. 2. TUNEL assays in normal, SCO and hypospermatogenic testes. *In situ* TUNEL assay and immunofluorescent localization of NDRG2 and DAPI in normal, congenital SCO, secondary SCO and hypospermatogenic testes. These sections were visualized using TUNEL (green), TRITC (red), and DAPI (blue). Confocal images indicate that NDRG2 immunoreactivity was present mainly in the cytoplasm of Leydig cells in testes of normal spermatogenesis, while the signal for NDRG2 also resided in apoptotic Leydig cells, germ cells and Sertoli cells in hypospermatogenic and both types of SCO testes. Colocalization of NDRG2 immunoreactivity (red) with TUNEL labeling (green) and DAPI (blue) is indicated by white color in the overlay image. Arrows: Leydig cells with TUNEL, NDRG2, and DAPI signal in the nucleus; solid arrowheads: Leydig cells with cytoplasmic NDRG2 staining and nuclear DAPI staining; open arrowheads: Sertoli cells with TUNEL, NDRG2 and DAPI signal in the nucleus; dual arrowheads: germ cells with TUNEL, NDRG2 and DAPI signal in the nucleus. Data represent groups of patients (normal, n = 8; congenital SCO, n = 6; secondary SCO, n = 5; hypospermatogenesis, n = 6) (scale bars 50 μm).

in Leydig cell and Sertoli cell nuclei in testes of both types of SCO (Fig. 1B). Relatively intensive NF-κB staining was found in the interstitial Leydig cells of testes with normal and abnormal spermatogenesis (Fig. 1C). The positive NF-κB staining in the seminiferous tubules was confined to the nuclei of Sertoli cells and germ cells of testes of both types of SCO and hypospermatogenesis (Fig. 1C). Table 1 listed all the positive staining rate of NDRG2 and NF-κB in Leydig cells of congenital SCO, secondary SCO, hypospermatogenesis and normal testes.

The absence of TUNEL staining in normal testes was accompanied by restricted expression of NDRG2 only in the cytoplasm of Leydig cells. TUNEL assays also confirmed the immunohistochemistry results that NDRG2 was localized in the apoptotic Leydig cells, Sertoli cells and germ cells, as intensive staining for TUNEL and NDRG2 colocalized in the DAPI-labeled nuclei of such cells (Fig. 2). For patients Leydig cell apoptosis rate, see Table 1.

3.2. Expression of NDRG2 and NF-κB in EDS-treated murine testes

Exposure to EDS gradually eliminates Leydig cells from rat testis for 72 h [8,10,11,30], so it was used in this study to mimic Leydig cell apoptosis. In the testes with intraperitoneal EDS (75 mg/kg) administration, HE staining and real-time PCR results indicated rat Leydig cell hypoplasia (Fig. 3A and B). Leydig cells started to degenerate gradually at 2 h after EDS treatment (98.93% as many Leydig cells as control group) (Fig. 3A and B). Twenty-four hours later, this ratio dropped to 28.54% (Fig. 3A and B). Finally, 72 h post–EDS treatment, Leydig cells almost disappeared (8.35% compared to control group) (Fig. 3A and B). However, after PDTC (100 mg/kg) and EDS treatment for 72 h, Leydig cells had been protected from apoptosis (97.85% compared to control group) (Fig. 3A and B). Immunohistochemistry demonstrated that in control testes, NDRG2 was found mainly in the cytoplasm of Leydig cells (Fig. 4A), as observed in human testes with normal spermatogenesis. As described in testes with hypospermatogenesis and SCO, intense staining of NDRG2 was detected in the nuclei of apoptosis-like Leydig cells and germ cells at 6 h to 48 h post-EDS (Fig. 4A). Similar to NDRG2, NF-κB was also located in the cytoplasm and nuclei of Leydig cells and germ cells after EDS stimulation (Fig. 4B). These effects were also abolished by PDTC together with EDS injection (Fig. 4A and B). Furthermore, we examined the expression and distribution of NDRG2 and NF-κB in cultured TM3 cells treated with EDS (1.0 mg/ml). NDRG2 and NF-κB immunoreactivity was located in the cytoplasm of healthy TM3 cells (see Section 3.4).

As described in hypospermatogenic and SCO testes, TUNEL and immunofluorescence staining for NDRG2 and 3β-HSD (marker of Leydig cells) were performed in the *in vivo* and *in vitro* models of apoptotic Leydig cells induced by EDS and/or PDTC. NDRG2 staining was localized predominantly in the cytoplasm of Leydig cells. Meanwhile, the colocalization of apoptotic cells (green), NDRG2-positive cells (red), and 3β-HSD–positive cells (blue) revealed that NDRG2 expression in apoptotic Leydig cells or cultured TM3 cells was induced by EDS administration (Fig. 5). In addition, at 6 h to 48 h post-EDS, NDRG2 staining could also be found in the nuclei of Leydig cells (Fig. 4A). As described in Section 3.1, apoptotic germ cells were observed at 6 h, 12 h, and at their peak 24 h post-EDS, some of which had positive signal representing NDRG2, indicated by yellow color (Fig. 5). Nevertheless, simultaneous administration of PDTC and EDS dramatically reduced Leydig and germ cell apoptosis, as indicated by the absence of TUNEL signal in the testis (Fig. 5). For results of different doses of EDS treated mice testicular structures, NDRG2 and NF-κB localization, see Supplementary Fig. 3.

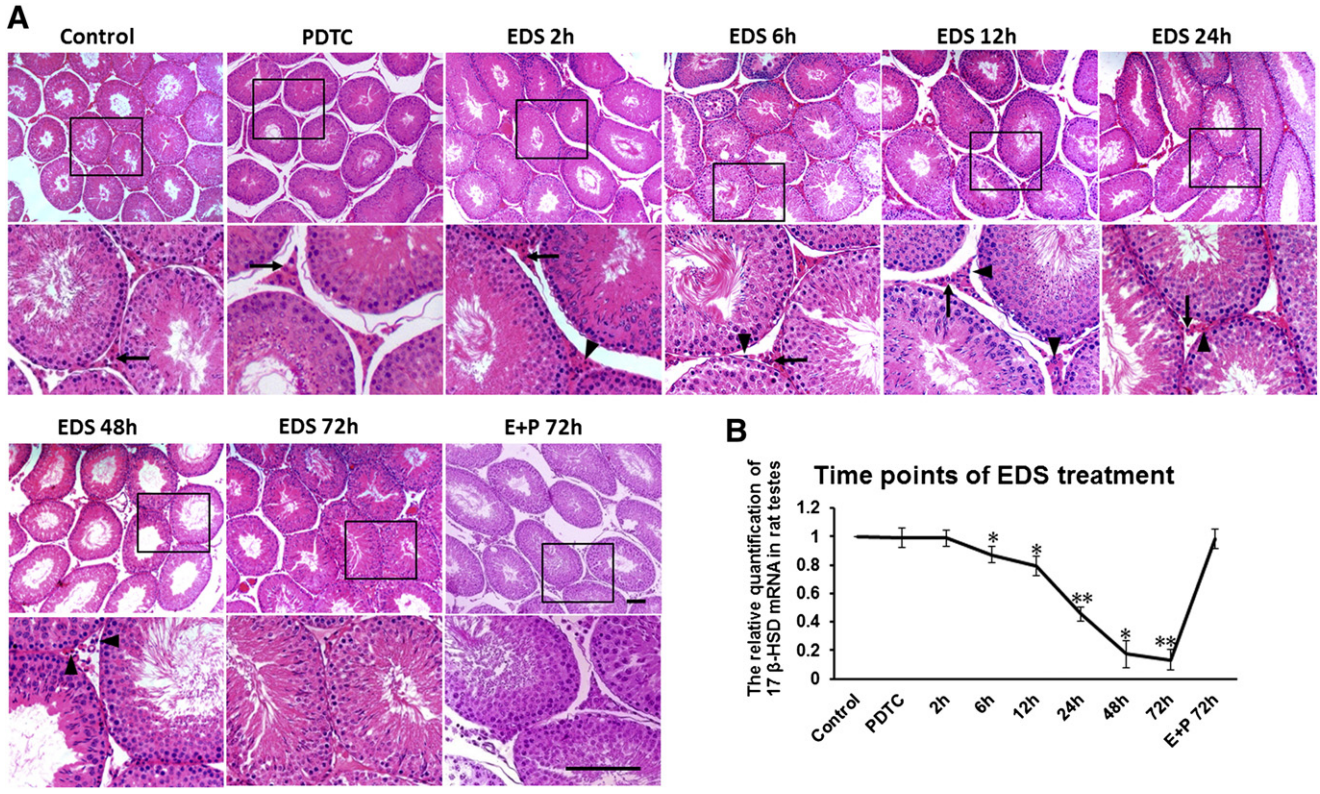

Fig. 3. Testicular structure of EDS- and/or PDTC-treated testes. (A) HE staining of a vehicle control SD rat and rats 2 h, 6 h, 12 h, 24 h, 48 h and 72 h after intraperitoneal administration of 75 mg/kg EDS (vehicle used for EDS, DMSO:H_2O = 1:3) and/or PDTC (100 mg/kg, diluted in H_2O). Leydig cells show condensation of the nuclear chromatin, a morphological sign of apoptosis, 6 h post-EDS treatment. Addition of PDTC for 72 h protected Leydig cell viability, as confirmed by the restored Leydig cell number in the interstitial tissue compared with testis 72 h post-EDS treatment. Both sections show two images at lower and higher magnification, respectively. Arrows: healthy Leydig cells; arrowheads: apoptotic Leydig cells. Data represent groups of rats (n = 5 per group) (scale bars 50 μm). (B) Linear chart representing relative mRNA level of *17β-HSD* III, marker of adult Leydig cell, after EDS and/or PDTC treatment. Data are presented as mean ± SEM and are representative of three independent experiments in each group (n = 5 per group) (*P < 0.05, **P < 0.01 compared to the control group, one-way ANOVA).

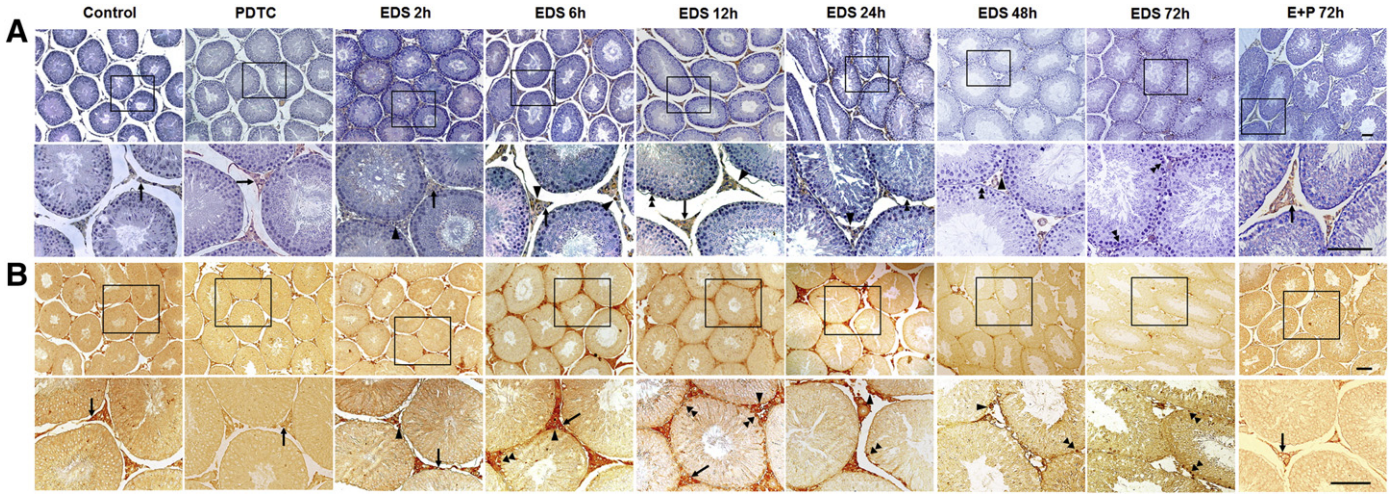

Fig. 4. NDRG2 and NF-κB expression in EDS- and/or PDTC-treated rat testes. (A) Immunolocalization of NDRG2 expression in the testis of control rats and rats sacrificed after 75 mg/kg EDS and/or 100 mg/kg PDTC treatment. In the control and PDTC (±EDS)-treated testis, NDRG2 was localized in the cytoplasm of the Leydig cells, while after only EDS administration, the signal for NDRG2 appeared in the nuclei of Leydig cells and germ cells with condensed nuclear chromatin. (B) NF-κB expression in testis after EDS and/or PDTC treatment. In the control and PDTC (±EDS)-treated testis, NF-κB was mainly localized in the cytoplasm of the Leydig cells and spermatogonia. After simply EDS stimulation, signal for NF-κB appeared in the nuclei of Leydig cells and spermatogonia with condensed nuclear chromatin. Both sections show two images at lower and higher magnification, respectively. Arrows: Leydig cells with positive signal for NDRG2 or NF-κB only in cytoplasm; arrowheads: Leydig cells with positive signal for NDRG2 or NF-κB both in cytoplasm and nucleus; dual arrowheads: germ cells with positive signal for NDRG2 or NF-κB. Data represent groups of rats (n = 5 per group) (scale bars 50 μm).

3.3. Up-regulation of NDRG2 in EDS-induced apoptotic Leydig cells

Annexin V/PI staining showed that EDS cytotoxicity increased with incubation time in Leydig cells. In TM3 cells, apoptotic cells constituted 1.7% in the control group and 25.65%, 33.57%, 35.68% and 39.40% in the 2 h, 6 h, 12 h and 24 h EDS-treated groups, respectively (Fig. 6A and B). However, the apoptotic rate of TM3 cells in the PDTC (200 μmol) plus EDS treatment group decreased to 1.6%, 1.9%, 2.5%, 2.7% and 6.1%, from 2 h to 24 h post-treatment, respectively (Fig. 6A and B), which suggests that *in vitro* Leydig cell apoptosis triggered by EDS could be alleviated by blocking NF-κB.

To further analyze the dynamic pattern of NDRG2 expression in apoptotic Leydig cells *in vivo*, western blot and real-time quantitative PCR were performed in lysates of purified Leydig cells collected from testes 2 h, 6 h, 12 h and 24 h after EDS treatment. The anti-NDRG2 immunoreactive band of about 42 kDa appeared similar to the vehicle-treated group 2 h post-EDS and started to increase in intensity during the next 22 h, finally reaching its peak at 24 h, when its intensity dramatically

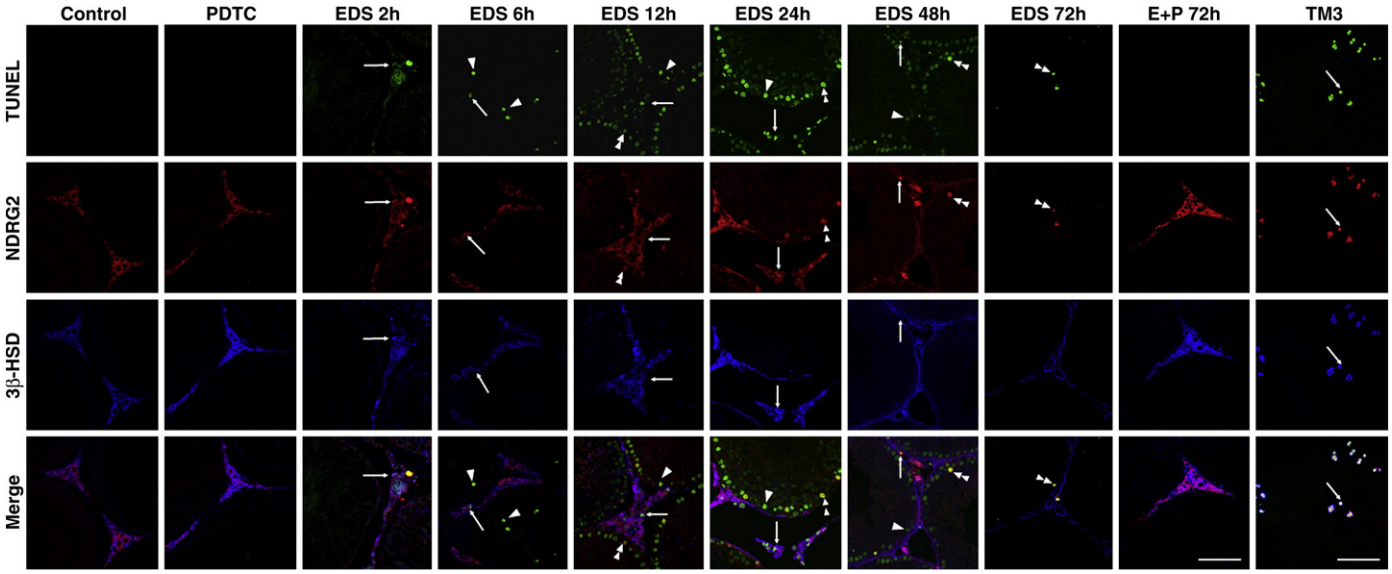

Fig. 5. TUNEL assays in testes and cells with EDS and/or PDTC treatment. Immunofluorescent localization of NDRG2 and 3β-HSD by *in situ* TUNEL assay for the presence of apoptotic cells in the testis of adult rats before and 2 h, 6 h, 12 h, 24 h, 48 h and 72 h after 75 mg/kg EDS and/or 100 mg/kg PDTC treatment as well as cell slides incubated with 1.0 mg/ml EDS. These sections and cell slides were visualized using TUNEL (green), TRITC (red), and CY5 (blue). Confocal images indicate that NDRG2 immunoreactivity is present mainly in 3β-HSD-containing Leydig cells in the EDS and/or PDTC groups, while the signal for NDRG2 also resided in apoptotic germ cells 12 h to 72 h post-EDS. Colocalization of NDRG2 immunoreactivity (red) with TUNEL labeling (green) or a 3β-HSD-positive signal (blue) is indicated by yellow or pink color in the overlay image. Arrows: Leydig cells with TUNEL and NDRG2 nuclear labeling as well as cytoplasmic 3β-HSD signal; Arrowheads: germ cells with TUNEL labeling in nucleus; dual arrowheads: germ cells with TUNEL and NDRG2 signal in the nucleus. Data represent groups of rats (n = 5 per group) (scale bars 50 μm in testicular sections, 20 μm in TM3 cell slides).

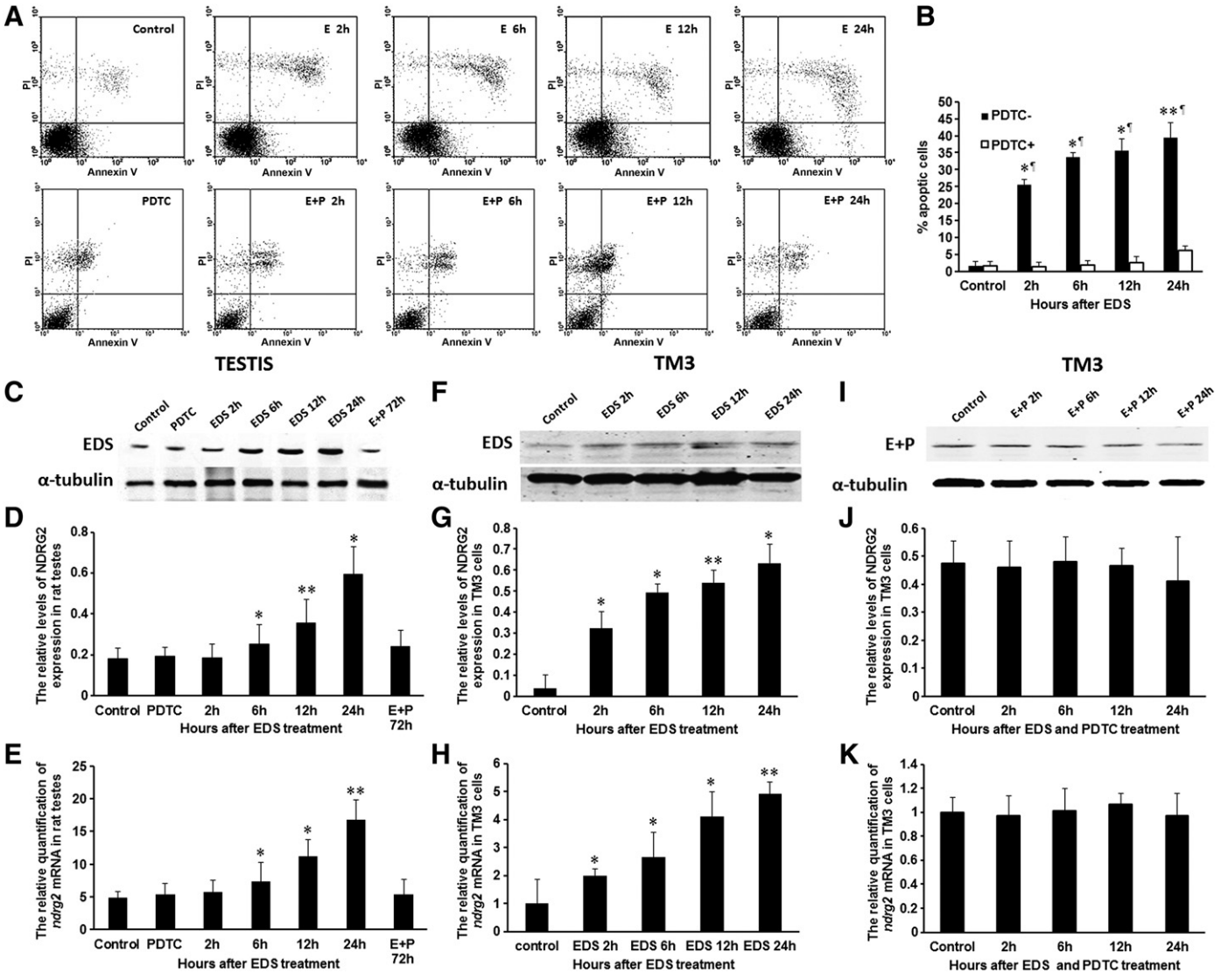

Fig. 6. Apoptosis of TM3 cells and dynamics of NDRG2 expression after exposure to EDS. (A, B) FACS scan results indicate the apoptosis rate after TM3 cells were incubated with culture medium containing vehicle, 200 μmol PDTC and/or 1.0 mg/ml EDS for 2 h, 6 h, 12 h or 24 h. The percentage of apoptotic cells in the EDS group are 1.7% for vehicle treatment, 25.65% for 2 h EDS, 33.57% for 6 h, 35.68% for 12 h, and 39.40% for 24 h. The percentage of apoptotic cells in the PDTC + EDS group are 1.6%, 1.9%, 2.5%, 2.7% and 6.1%, from 2 h to 24 h post treatment, respectively. (C, D) Western blot and histogram for NDGR2 expression in lysates of purified Leydig cells after exposure to vehicle, EDS and/or PDTC. (F, G) Western blot and histogram for NDGR2 expression in whole-cell lysates from TM3 cells incubated with culture medium containing vehicle or EDS. (I, J) Western blot and histogram for NDGR2 expression in whole-cell lysates from TM3 cells incubated with culture medium containing PDTC and/or EDS. α-Tubulin served as internal control. (E, H, K) Real-time PCR using RNA collected from the above tissue and cell samples. Data are presented as mean ± SEM and are representative of three independent experiments of each group (n = 5 per group) (*P<0.05, **P<0.01 compared to the control group, ¶P<0.05, two-way ANOVA).

exceeded the control group (Fig. 6C and D). Furthermore, we investigated TM3 cells 2 h, 6 h, 12 h and 24 h post–EDS treatment. The relative protein level of NDRG2 increased 2 h after the EDS exposure and reached its peak at 24 h, in agreement with the *in vivo* model (Fig. 6F and G). However, the relative level of NDRG2 when PDTC was intraperitoneally injected or added into the culture medium remained constant from 2 h to 24 h (Fig. 6C, D, I and J). The PCR results were consistent with western blot analysis (Fig. 6E, H and K). These results combined with quantification of apoptosis by flow cytometer corroborate the finding that the protein level of *ndrg2* was elevated in apoptotic Leydig cells, which could be blocked by PDTC.

3.4. Nuclear translocation of NDRG2 and NF-κB in EDS-induced apoptotic Leydig cells

The activation and translocation of NF-κB and NDRG2 in EDS-induced apoptotic Leydig cells were measured by immuno-fluorescence and western blot. FITC-labeled NF-κB and TRITC-labeled NDRG2 signal were detected in the nuclei of most Leydig cells after incubation with EDS (1.0 mg/ml) or TNF-α (100 ng/ml, as positive control) for 2 h (Fig. 7A). In the vehicle-treated groups, NF-κB and NDRG2 remained in the cytoplasm (Fig. 7A). In addition, nuclear protein was extracted after TM3 cells were treated with EDS, TNF-α or vehicle for 30 min, 1 h, or 2 h. The relative levels of NDRG2 and NF-κB increased from 30 min to 2 h in the EDS-stimulated nuclei, while they remained nearly constant in the TNF-α group (Fig. 7B and C). Meanwhile, the expression of NF-κB and NDRG2 in the cytoplasm extracts confirmed our earlier results that NDRG2 was up-regulated in both the cytoplasm and nuclear extracts after 30 min to 2 h exposure to EDS, while NF-κB level in the cytoplasm was decreasing, possibly due to the nuclear translocation (Fig. 7D and E). Addition of vehicle abolished such translocation (Fig. 7D and E). These results suggest that NF-κB and NDRG2 translocated into the nucleus under stimulation by EDS or TNF-α.

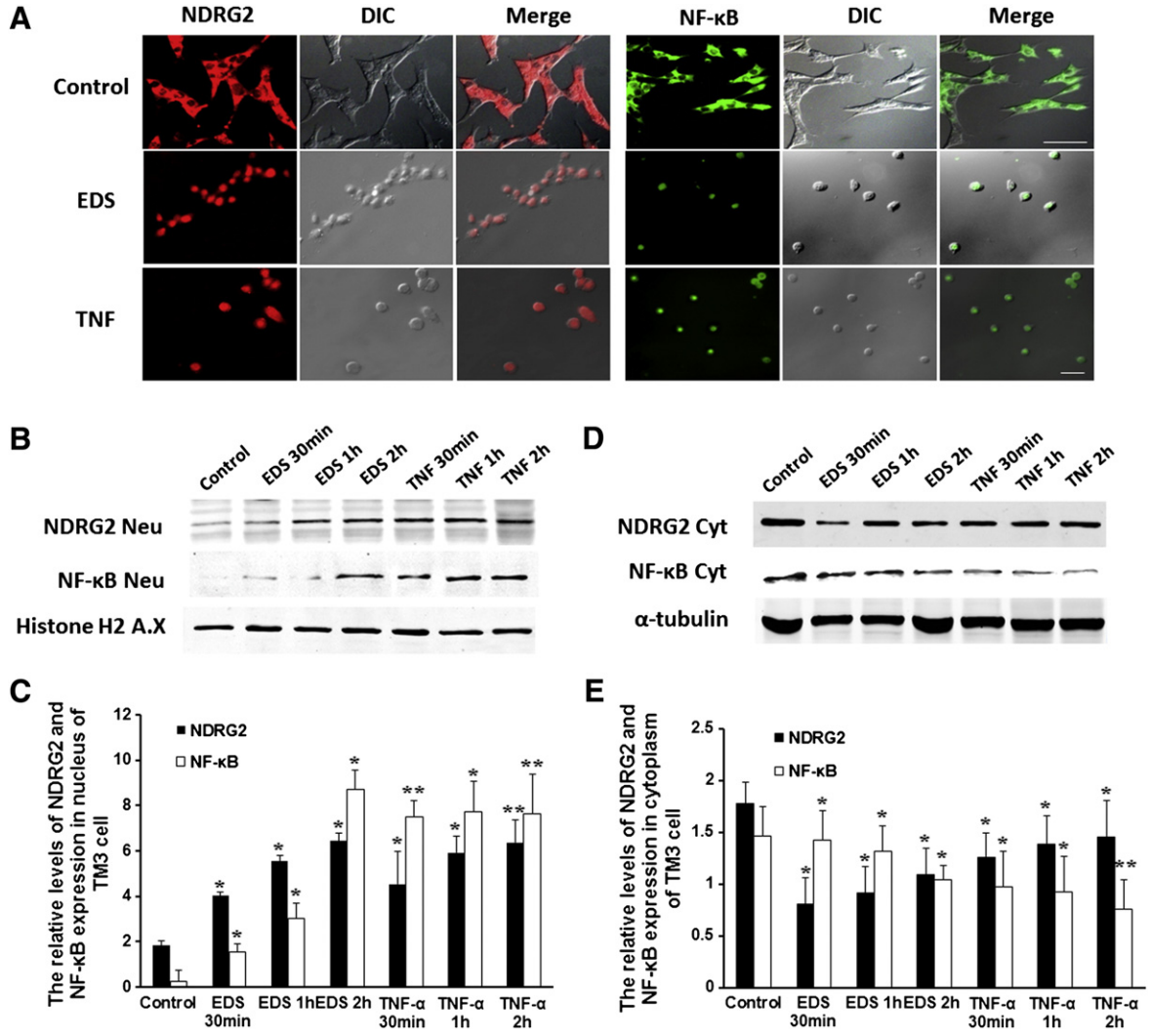

Fig.7. Nuclear translocation of NDRG2 and NF-κB in TM3 cells. (A) Differential interference contrast (DIC) and immunofluorescent staining using TRITC (red) and FITC (green) to represent NDRG2 (TRITC) and NF-κB (FITC) expression revealed NDRG2 and NF-κB translocated into the nucleus after incubation with medium containing 1.0 mg/ml EDS or 100 ng/ml TNF-α, but they did not in the control group (scale bars 10 μm). (B, C) The relative protein levels of NDRG2 and NF-κB were increased compared to the control group in nuclear protein extracts of cells treated with EDS, but not TNF-α, as characterized by western blot using antibodies against NDRG2 and NF-κB. Histone H2A.X served as internal control for nuclear extracts. (D, E) The relative protein level of NF-κB in cytoplasm decreased when cells were stimulated by EDS, but not TNF-α, while the relative level of NDRG2 slightly increased in the EDS group. α-Tubulin served as internal control. Data are presented as mean ± SEM and are representative of three independent experiments of each group (n = 5 per group) (*P<0.05, **P<0.01 compared to the control group, one-way ANOVA).

3.5. Modulation of NF-κB on the mouse NDRG2 promoter through conjugation to its putative binding sites

Analysis of the −1943 bp to +250 bp region of the *ndrg2* gene sequence, which contains the majority of the *ndrg2* promoter region, confirmed the presence of five motifs that resembled the general consensus binding site of NF-κB members (Fig. 8C). Thus, transient transfection in the TM3 cell line was utilized to analyze whether NF-κB could modulate transcription from the mouse *ndrg2* promoter. The basic relative promoter activity of full-length (−1943 bp to +249 bp) mouse *ndrg2* promoter was significantly higher than truncated promoters when TM3 cells were stimulated by TNF-α or EDS for 8 h (Fig. 8B). The incubation time was based on our preliminary experiments with TNF-α or EDS stimulation for 2 h, 4 h, 6 h, 8 h, which showed that the promoter activity was highest at 8 h (data not shown). Deletion of bp −1943 to −210 by Kpn I digestion completely abrogated the transcriptional activation triggered by NF-κB (Fig. 8B). This indicates the absence of effective NF-κB-responsive motifs between bp −210 and +249, as the putative binding sites in this region only exist on a single strand of DNA, while other putative sites are predicted to be equally strong on both strands. In addition, deletion of −1943 bp to −1463 bp, −1943 bp to −995 bp, −1943 bp to −449 bp significantly reduced transcriptional activity of *luc*, possibly due to the loss of functional NF-κB binding sites (Fig. 8B). Addition of PDTC eliminated the differences in the promoter activities of the EDS, TNF-α and control groups, further supporting that NDRG2 is a regulator of apoptosis and is transcriptionally activated by NF-κB (Fig. 8B).

ChIP was used to confirm the conjugation of NF-κB to the NDRG2 promoter. The PCR results, in agreement with the luciferase reporter gene assay, indicated the binding of NF-κB to four putative binding sites in the NDRG2 promoter, while PDTC groups and negative control groups that received normal IgG or anti-α-tubulin antibody showed no such binding (Fig. 8A).

3.6. NDRG2 inhibition attenuates EDS-induced TM3 cell apoptosis and promotes cell growth

By blocking NDRG2 expression with siRNA, NDRG2 expression decreased about 60% as detected by western blot (Fig. 9A and B). Analysis of these samples with activated caspase-3 antibody demonstrated

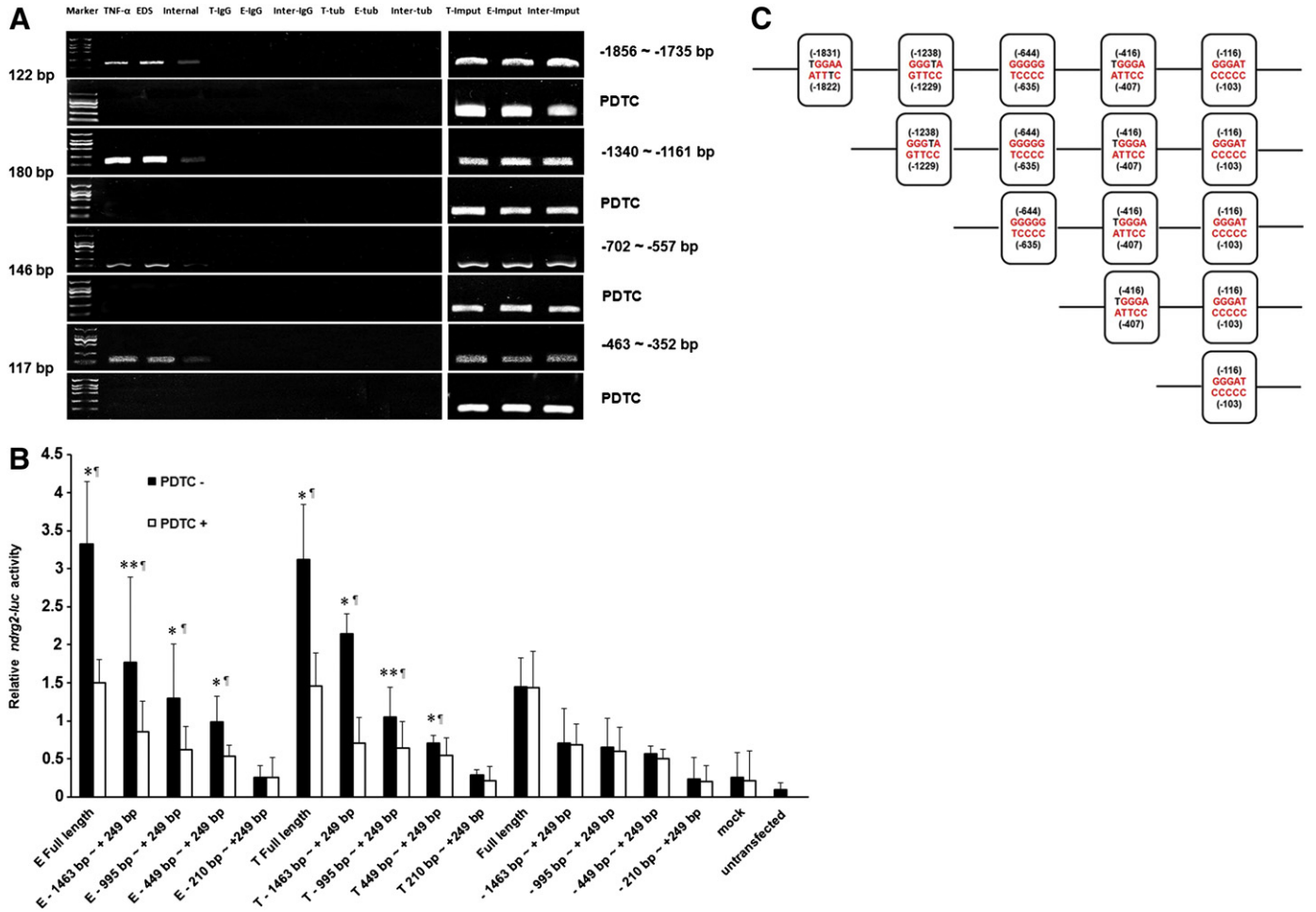

Fig. 8. NF-κB binding activity to the *ndrg2* promoter in response to EDS and TNF-α. (A) Detection of NF-κB binding in the *ndrg2* promoter in response to 1.0 mg/ml EDS, 100 ng/ml TNF-α or 200 μmol PDTC in TM3 cells by ChIP. Specific primers to the *ndrg2* promoter amplified regions containing NF-κB binding sites. The input represents the amplification of the unprecipitated DNA. PCR amplification of irrelevant immunoprecipitates with anti-α-tubulin antibody and normal rabbit IgG were used as negative controls. (B) Elevation of NF-κB-dependent *ndrg2* transcriptional activity induced by EDS and TNF-α in TM3 cells. Cells were co-transfected with pGL3-mouse *ndrg2* promoter-*luc* or a pGL3-mouse *ndrg2* truncated promoter-*luc* construct along with the phRL-SV40 Renilla before treatment with EDS, TNF-α and/or PDTC, followed by lysis and luminescence detection. The relative *ndrg2* transcriptional activity of the full-length mouse *ndrg2* promoter stimulated by both EDS and TNF-α was reduced through truncation and addition of PDTC. (C) Putative NF-κB binding sites in the mouse *ndrg2* promoter region. Altogether, 5 putative binding sequences of NF-κB are located in the mouse *ndrg2* promoter region: −1831 to −1822, −1238 to −1229, −644 to −635, −416 to −407, and −116 to −103. These sequences were analyzed by promoter-analyzing software, with the consensus NF-κB binding sequence GGGRNNYYCC (N = any base, R = purine, Y = pyrimidine) as reference (red characters indicate bases of the promoter consistent with the consensus sequence), and finally cloned into the pGL3 vector. Data are mean ± SEM of relative luciferase: Renilla activity (relative light units) for 4 determinations (*P<0.05, **P<0.01 compared to the control group, ¶P<0.05, two-way ANOVA).

significantly decreased expression compared to the control group, while the relative level of total caspase-3 remained the same (Fig. 9A and B).

The extent of apoptosis after NDRG2 knock-down was quantified by flow-cytometric analysis in which TM3 cell lines were labeled with Annexin V and PI. Incubation with EDS for 18 h induced 21.37% and 7.78% apoptotic TM3 cells in the non-silencing control and RNAi groups, respectively, while the vehicle-treated RNAi group showed 1.09% apoptotic cells, as compared to 1.23% in the vehicle-treated non-silencing control group (Fig. 9C and D).

DNA amplification was measured by EdU staining and detected by confocal imaging. The results indicate that NDRG2 knock-down in EDS-exposed groups increased the amount of proliferating cells 7.61% as compared to the non-silencing control groups, whereas in vehicle-treated groups, such effect was not observed (Fig. 9E and F).

3.7. NDRG2 over-expression aggravates EDS-induced TM3 cell apoptosis and inhibits cell growth

To trigger NDGR2 over-expression, pcDNA3.1-*ndrg2* was transfected into TM3 cells. Western blot indicated that the relative protein level of NDRG2 was up-regulated by 40% (Fig. 9A and B). Active caspase-3 increased compared to the control group, while total caspase-3 remained unaltered (Fig. 9A and B).

Flow cytometry was performed to measure the apoptotic rate after over-expression of NDRG2. NDRG2-over-expressing and non-silencing siRNA transfected TM3 cells exposed to EDS for 18 h showed 62.46% and 21.37% apoptotic cells, respectively, while the vehicle-treated NDRG2 over-expression group had 30.58% apoptotic cells, compared to 1.23% in the vehicle-treated non-silencing control group (Fig. 9C and D).

EdU staining further demonstrated that over-expression of NDRG2 in vehicle or EDS-treated cells induced 23.72% or 28.39% fewer proliferating cells, respectively, than without NDRG2 over-expression (Fig. 9E and F).

4. Discussion

Apoptosis of Leydig cells, the main generator of testosterone production *in vivo*, is characterized by the activation of the Fas/Fas ligand system under certain circumstances [4–7]. Leydig cell apoptosis can

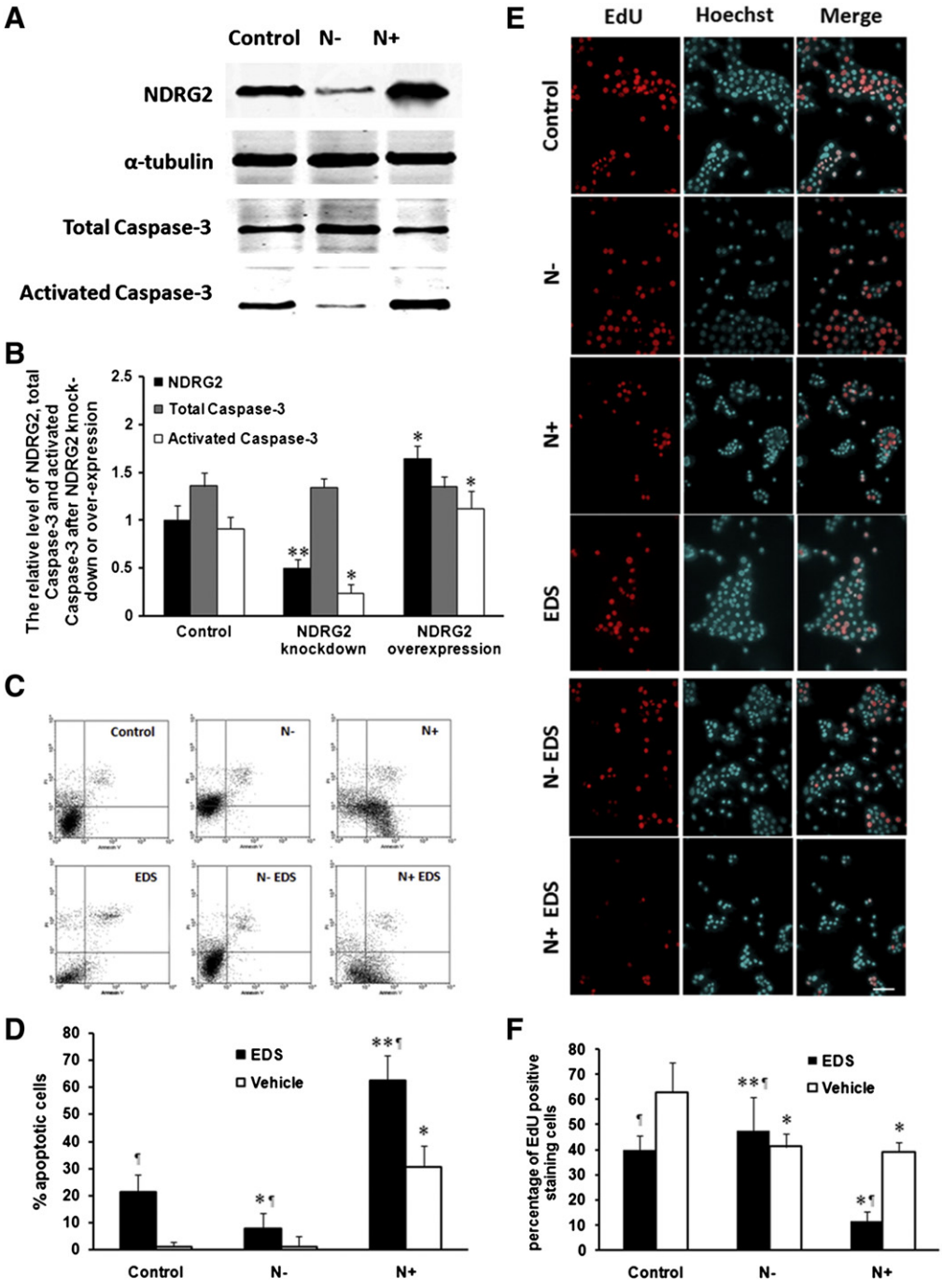

Fig. 9. Effects of NDRG2 knock-down and over-expression on TM3 cell proliferation and apoptosis. (A, B) NDRG2, total caspase-3, and activated caspase-3 expression after TM3 cells were transfected with *ndrg2*-siRNA (N−) or *ndrg2*-pcDNA 3.1 plasmid (N+), as characterized by western blot. α-Tubulin was used as loading control. (C, D) FACS scan results indicate the percentage of apoptotic TM3 cells induced by 1.0 mg/ml EDS stimulation after NDRG2 knock-down or over-expression. The percentage of apoptotic cells is 1.09% for *ndrg2*-RNAi, 30.58% for NDRG2 over-expression, 7.78% for EDS-treated *ndrg2*-RNAi, 62.46% for EDS-treated NDRG2 over-expression, 21.37% for EDS, and 1.23% for vehicle-treated untransfected cells. (E, F) NDRG2 knock-down promoted and over-expression inhibited Leydig cell growth *in vitro*. TM3 cells were transfected with *ndrg2*-pcDNA 3.1 or *ndrg2*-siRNA, and then incubated with either vehicle or EDS solution. The proliferative percentages in the vehicle group are 62.92% for untransfected cells and 39.2% and 41.24% for NDRG2 over-expression and knock-down, respectively, compared to 39.86% for EDS-treated untransfected cells and 11.47% and 47.48% for EDS-treated NDRG2 over-expression and knock-down, respectively. Data are presented as mean ± SEM. Data are representative of three independent experiments of each group (n = 5 per group) (*P < 0.05 compared to the control group, ¶P < 0.05, two-way ANOVA).

also be found in testicular biopsies of SCO, MA and hypospermatogenesis patients [3]. Accordingly, EDS-induced Leydig cell apoptosis is a consequence of Fas system activation [10,11]. Leydig cell apoptosis is not related to p53 activation due to its extremely low transcriptional activity [35], but activation of NF-κB participates glucocorticoid induced Leydig cell apoptosis [26]. However, the molecular mechanism of Leydig cell apoptosis is still not fully understood. Here, we showed that in Leydig cells, NDRG2, regulated by NF-κB, is essential for cell death under the stress of pro-apoptotic factors and, for the first time to our knowledge, investigated the activity of NF-κB at the *ndrg2* gene promoter.

Ndrg2 was traditionally considered a putative tumor suppressor gene that could repress the growth of several tumor cell lines [15–20,24,36–39]. Moreover, it is involved in p53- and HIF-related apoptosis [21,22]. NDRG2 is expressed in Leydig cells in human testes

with normal spermatogenesis [12]. However, little is known about the expression of NDRG2 in infertile testes. As we explored NDRG2 expression in infertile testes, we found that NDRG2 not only is expressed in the cytoplasm of normal Leydig cells but also translocates into the nuclei of apoptotic Leydig cells, Sertoli cells and germ cells. To further elucidate NDRG2's functions in this process, EDS was used to specifically induce Leydig cell degeneration. HE staining, immunohistochemistry and immunofluorescence combined with TUNEL staining confirmed that NDRG2 is located only in the cytoplasm of healthy Leydig cells, while it is expressed in both the cytoplasm and the nuclei of EDS-induced rat apoptotic Leydig cells or TM3 cells. Accordingly, the expression of NDRG2 in apoptotic germ cells, as a result of androgen deprivation triggered by EDS-induced Leydig cell apoptosis, has been reported in MAA-induced germ cell apoptosis [12]. Nevertheless, further studies should be done to understand the mechanisms and effects of these expression changes.

NF-κB, a pro-apoptotic transcription factor, has been correlated with the apoptosis of both Leydig and germ cells [40–44], but it has not been shown to be involved in SCO, hypospermatogenesis or EDS-induced Leydig cell apoptosis. In fact, NF-κB can be activated through the Fas-stimulated activation of RIP-1 or pro-caspase-8 [25]. Thus, we hypothesized that NDRG2 is a regulator of apoptosis and is up-regulated by NF-κB. This hypothesis was supported by our identification of five elements in the *ndrg2* promoter region that were extremely similar to or conformed to the consensus NF-κB specific binding sequence, GGGRNNYYCC (N = any base, R = purine, Y = pyrimidine) [45] (Fig. 9C). NF-κB has a similar expression profile as NDRG2 in SCO, hypospermatogenesis and EDS-treated testes, while it is stage-specifically expressed in these testes [46]. *In vivo* and *in vitro* inhibition of NF-κB by PDTC blocked Leydig cell apoptosis and altered the NDRG2 expression profile. This intrigued us to further explore the regulation of NDRG2 by NF-κB in Leydig cells.

To the best of our knowledge, there are no studies showing that NDRG2 can be regulated by NF-κB. Here we report that under certain doses of TNF-α and EDS, NF-κB translocated into the nucleus. This implied that NF-κB could bind to the mouse *ndrg2* promoter region and regulate its expression. To confirm our hypothesis, luciferase assays and ChIP were used. The results confirmed that NF-κB was not merely activated by TNF-α and EDS, but it further elevated the relative transcriptional activity from the *ndrg2* promoter through conjugation to its −1831 bp to −1822 bp, −1238 bp to −1229 bp, −644 bp to −635 bp and −416 bp to −407 bp binding sites, which was abolished when truncated promoters were used or NF-κB was inhibited by PDTC. In addition to NF-κB, NDRG2 appeared in the nuclei of Leydig cells of SCO and hypospermatogenesis patients and cells treated with TNF-α or EDS. These findings were confirmed by TUNEL assays and western blots of nuclear extracts. In fact, NDRG2 can translocate into the nucleus under hypoxia stress, which is abolished by deleting amino acids 101 to 178 [21]. However, further studies should be done to understand the mechanisms and purposes of such translocation.

To confirm our findings were not constricted only to human and rat species, here we reported, for the first time within our knowledge, that a single injection of 375 mg/kg EDS triggered massive mouse Leydig cell loss *in vivo* (Supplementary Fig. 3). NDRG2 and NF-κB expression were also characterized in these testes (Supplementary Fig. 3). Nevertheless, additional experiments should be done to evaluate the difference between EDS mouse model and rat model.

Based on the previous postulation that NDRG2 might regulate Leydig cell apoptosis through up-regulation by NF-κB, we confirmed this connection by over-expression and knock-down of NDRG2. EDS-induced Leydig cell apoptosis was elevated and proliferation reduced by NDRG2 over-expression. As expected, NDRG2 knock-down caused the reverse effect. These findings suggest that NDRG2 might be a pivotal protein that participates cell apoptosis and partly explain the high expression of NDRG2 in apoptotic Sertoli cells and germ cells.

All together, these data suggest that *ndrg2* might be a pivotal gene that promotes Leydig cell apoptosis under NF-κB regulation. We postulate that EDS-induced Fas activation triggers detachment of NF-κB from IκB through RIP and/or pro-caspase-8. NF-κB then translocates into the nucleus and binds the promoter region of *ndrg2*, which further elevates the protein level of NDRG2. NDRG2 can then translocate back into the nucleus and have downstream effects, such as feedback toward NF-κB or regulation of downstream genes. Further analysis of NDRG2's functions in Sertoli cells and germ cells might reveal its role in fertility and sterility and whether similar effects of NF-κB's regulation of NDRG2 exist in other cells, organs and species.

Supplementary materials related to this article can be found online at doi:10.1016/j.bbadis.2011.11.013

Acknowledgements

This study was supported by the Natural Science Foundation of China (grants No. 30871309, No. 31171154, No. 30830054 and No. 31070681). Special thanks to Prof. Tian-Le Xu (Shanghai Jiao Tong University School of Medicine), Prof. Rui-An Wang, Dr. Guo-Dong Yang, Dr. Liang-Liang Shen and Dr. Zhen Li (Fourth Military Medical University) for their assistance.

References

[1] N. Ozawa, N. Goda, N. Makino, T. Yamaguchi, Y. Yoshimura, M. Suematsu, Leydig cell-derived heme oxygenase-1 regulates apoptosis of premeiotic germ cells in response to stress, J. Clin. Invest. 109 (2002) 457–467.
[2] S.B. Rulli, P. Ahtiainen, S. Mäkelä, J. Toppari, M. Poutanen, I. Huhtaniemi, Elevated steroidogenesis, defective reproductive organs, and infertility in transgenic male mice overexpressing human chorionic gonadotropin, Endocrinology 144 (2003) 4980–4990.
[3] S.K. Kim, Y.D. Yoon, Y.S. Park, J.T. Seo, J.H. Kim, Involvement of the Fas–Fas ligand system and active caspase-3 in abnormal apoptosis in human testes with maturation arrest and Sertoli cell-only syndrome, Fertil. Steril. 87 (2007) 547–553.
[4] K. Boekelheide, Mechanisms of toxic damage to spermatogenesis, J. Natl. Cancer Inst. Monogr. 2005 (2005) 6–8.
[5] H.B. Gao, M.H. Tong, Y.Q. Hu, Q.S. Guo, R. Ge, M.P. Hardy, Glucocorticoid induces apoptosis in rat Leydig cells, Endocrinology 143 (2002) 130–138.
[6] R. Sivakumar, P.B. Sivaraman, N. Mohan-Babu, I.M. Jainul-Abideen, P. Kalliyappan, K. Balasubramanian, Radiation exposure impairs luteinizing hormone signal transduction and steroidogenesis in cultured human leydig cells, Toxicol. Sci. 91 (2006) 550–556.
[7] T.T. Turner, H.J. Bang, J.J. Lysiak, Experimental testicular torsion: reperfusion blood flow and subsequent testicular venous plasma testosterone concentrations, Urology 65 (2005) 390–394.
[8] A.J. Morris, M.F. Taylor, I.D. Morris, Leydig cell apoptosis in response to ethane dimethanesulphonate after both *in vivo* and *in vitro* treatment, J. Androl. 18 (1997) 274–280.
[9] M.F. Taylor, I. Woolveridge, A.D. Metcalfe, C.H. Streuli, J.A. Hickman, I.D. Morris, Leydig cell apoptosis in the rat testes after administration of the cytotoxin ethane dimethanesulphonate: role of the Bcl-2 family members, J. Endocrinol. 157 (1998) 317–326.
[10] M.F. Taylor, M. de Boer-Brouwer, I. Woolveridge, K.J. Teerds, I.D. Morris, Leydig cell apoptosis after the administration of ethane dimethanesulfonate to the adult male rat is a Fas-mediated process, Endocrinology 140 (1999) 3797–3804.
[11] J.M. Kim, L. Luo, B.R. Zirkin, Caspase-3 activation is required for Leydig cell apoptosis induced by ethane dimethanesulfonate, Endocrinology 141 (2000) 1846–1853.
[12] W.G. Hou, Y. Zhao, L. Shen, J. Zhao, X.W. Liu, Z. Li, X.P. Liu, L.B. Yao, Y.Q. Zhang, Differential expression of N-Myc downstream regulated gene 2 (NDRG2) in the rat testis during postnatal development, Cell Tissue Res. 337 (2009) 257–267.
[13] X.L. Hu, X.P. Liu, Y.C. Deng, S.X. Lin, L. Wu, J. Zhang, L.F. Wang, X.B. Wang, X. Li, L. Shen, Y.Q. Zhang, L.B. Yao, Expression analysis of the NDRG2 gene in mouse embryonic and adult tissues, Cell Tissue Res. 325 (2006) 67–76.
[14] L. Yao, J. Zhang, X. Liu, NDRG2: a Myc-repressed gene involved in cancer and cell stress, Acta Biochim. Biophys. Sin. (Shanghai) 40 (2008) 625–635.
[15] J.J. Ma, C.G. Liao, X. Jiang, H.D. Zhao, L.B. Yao, T.Y. Bao, NDRG2 suppresses the proliferation of clear cell renal cell carcinoma cell A-498, J. Exp. Clin. Cancer. Res. 29 (2010) 103.
[16] Y. Deng, L. Yao, L. Chau, S.S. Ng, Y. Peng, X. Liu, W.S. Au, J. Wang, F. Li, S. Ji, H. Han, X. Nie, Q. Li, H.F. Kung, S.Y. Leung, M.C. Lin, N-Myc downstream-regulated gene 2 (NDRG2) inhibits glioblastoma cell proliferation, Int. J. Cancer 106 (2003) 342–347.
[17] X.L. Hu, X.P. Liu, S.X. Lin, Y.C. Deng, N. Liu, X. Li, L.B. Yao, NDRG2 expression and mutation in human liver and pancreatic cancers, World J. Gastroenterol. 10 (2004) 3518–3521.
[18] N. Liu, L. Wang, X. Liu, Q. Yang, J. Zhang, W. Zhang, Y. Wu, L. Shen, Y. Zhang, A. Yang, H. Han, J. Zhang, L. Yao, Promoter methylation, mutation, and genomic

deletion are involved in the decreased NDRG2 expression levels in several cancer cell lines, Biochem. Biophys. Res. Commun. 358 (2007) 164–169.
[19] E.A. Lusis, M.A. Watson, M.R. Chicoine, M. Lyman, P. Roerig, G. Reifenberger, D.H. Gutmann, A. Perry, Integrative genomic analysis identifies NDRG2 as a candidate tumor suppressor gene frequently inactivated in clinically aggressive meningioma, Cancer Res. 65 (2005) 7121–7126.
[20] Y. Park, S.K. Shon, A. Kim, K.I. Kim, Y. Yang, D.H. Cho, M.S. Lee, J.S. Lim, SOCS1 induced by NDRG2 expression negatively regulates STAT3 activation in breast cancer cells, Biochem. Biophys. Res. Commun. 363 (2007) 361–367.
[21] L. Wang, N. Liu, L. Yao, F. Li, J. Zhang, Y. Deng, J. Liu, S. Ji, A. Yang, H. Han, Y. Zhang, J. Zhang, W. Han, X. Liu, NDRG2 is a new HIF-1 target gene necessary for hypoxia-induced apoptosis in A549 cells, Cell. Physiol. Biochem. 21 (2008) 239–250.
[22] N. Liu, L. Wang, X. Li, Q. Yang, X. Liu, J. Zhang, J. Zhang, Y. Wu, S. Ji, Y. Zhang, A. Yang, H. Han, L. Yao, N-Myc downstream-regulated gene 2 is involved in p53-mediated apoptosis, Nucleic Acids Res. 36 (2008) 5335–5349.
[23] S.C. Choi, S.R. Yoon, Y.P. Park, E.Y. Song, J.W. Kim, W.H. Kim, Y. Yang, J.S. Lim, H.G. Lee, Expression of NDRG2 is related to tumor progression and survival of gastric cancer patients through Fas-mediated cell death, Exp. Mol. Med. 39 (2007) 705–714.
[24] A. Kim, M.J. Kim, Y. Yang, J.W. Kim, Y.I. Yeom, J.S. Lim, Suppression of NF-kappa B activity by NDRG2 expression attenuates the invasive potential of highly malignant tumor cells, Carcinogenesis 30 (2009) 927–936.
[25] S. Kreuz, D. Siegmund, J.J. Rumpf, D. Samel, M. Leverkus, O. Janssen, G. Häcker, O. Dittrich-Breiholz, M. Kracht, P. Scheurich, H. Wajant, NF-kappa B activation by Fas is mediated through FADD, caspase-8, and RIP and is inhibited by FLIP, J. Cell Biol. 166 (2004) 369–380.
[26] Q. Wang, H.B. Gao, Involvement of nuclear factor-kappa B on corticosterone-induced rat Leydig cell apoptosis, Asian J. Androl. 8 (2006) 693–702.
[27] R. Anniballo, F. Ubaldi, L. Cobellis, M. Sorrentino, L. Rienzi, E. Greco, J. Tesarik, Criteria predicting the absence of spermatozoa in the Sertoli cell-only syndrome can be used to improve success rates of sperm retrieval, Hum. Reprod. 15 (2000) 2269–2277.
[28] Y.O. Ilbey, E. Ozbek, A. Simsek, M. Cekmen, A. Otunctemur, A. Somay, Chemoprotective effect of a nuclear factor-kappa B inhibitor, pyrrolidine dithiocarbamate, against cisplatin-induced testicular damage in rats, J. Androl. 30 (2009) 505–514.
[29] Y. Zhao, W.G. Hou, H.P. Zhu, J. Zhao, R.A. Wang, R.J. Xu, Y.Q. Zhang, Expression of thyrotropin-releasing hormone receptors in rat testis and their role in isolated Leydig cells, Cell Tissue Res. 334 (2008) 283–294.
[30] F.F. Rommerts, L. Kuhne, G.W. van Cappellen, D.M. Stocco, S.R. King, A. Jankowska, Specific dose-dependent effects of ethane 1,2-dimethanesulfonate in rat and mouse Leydig cells and non-steroidogenic cells on programmed cell death, J. Endocrinol. 181 (2004) 169–178.
[31] Y. Zang, X.H. He, W.J. Xin, R.P. Pang, X.H. Wei, L.J. Zhou, Y.Y. Li, X.G. Liu, Inhibition of NF-kappa B prevents mechanical allodynia induced by spinal ventral root transection and suppresses the re-expression of Nav1.3 in DRG neurons *in vivo* and *in vitro*, Brain Res. 1363 (2010) 151–158.
[32] P.J. O' Shaughnessy, L. Willerton, P.J. Baker, Changes in Leydig cell gene expression during development in the mouse, Biol. Reprod. 66 (2002) 966–975.
[33] J. Vandesompele, K. De Preter, F. Pattyn, B. Poppe, N. Van Roy, A. De Paepe, F. Speleman, Accurate normalization of real-time quantitative RT-PCR data by geometric averaging of multiple internal control genes, Genome Biol. 3 (2002) R0034.
[34] P. Mestdagh, P. Van Vlierberghe, A. De Weer, D. Muth, F. Westermann, F. Speleman, J. Vandesompele, A novel and universal method for microRNA RT-qPCR data normalization, Genome Biol. 10 (2009) R64.
[35] J.Y. Chung, J.Y. Kim, Y.J. Kim, S.J. Jung, J.E. Park, S.G. Lee, J.T. Kim, S. Oh, C.J. Lee, Y.D. Yoon, Y.H. Yoo, J.M. Kim, Cellular defense mechanisms against benzo[a]pyrene in testicular Leydig cells: implications of p53, aryl-hydrocarbon receptor, and cytochrome P450 1A1 status, Endocrinology 148 (2007) 6134–6144.
[36] H. Furuta, Y. Kondo, S. Nakahata, M. Hamasaki, S. Sakoda, K. Morishita, NDRG2 is a candidate tumor-suppressor for oral squamous-cell carcinoma, Biochem. Biophys. Res. Commun. 391 (2010) 1785–1791.
[37] H. Shi, N. Li, S. Li, C. Chen, W. Wang, C. Xu, J. Zhang, H. Jin, H. Zhang, H. Zhao, W. Song, Q. Feng, X. Feng, X. Shen, L. Yao, Q. Zhao, Expression of NDRG2 in esophageal squamous cell carcinoma, Cancer Sci. 101 (2010) 1292–1299.
[38] H. Shi, H. Jin, D. Chu, W. Wang, J. Zhang, C. Chen, C. Xu, D. Fan, L. Yao, Suppression of N-myc downstream-regulated gene 2 is associated with induction of Myc in colorectal cancer and correlates closely with differentiation, Biol. Pharm. Bull. 32 (2009) 968–975.
[39] S.K. Shon, A. Kim, J.Y. Kim, K.I. Kim, Y. Yang, J.S. Lim, Bone morphogenetic protein-4 induced by NDRG2 expression inhibits MMP-9 activity in breast cancer cells, Biochem. Biophys. Res. Commun. 385 (2009) 198–203.
[40] K. Mizuno, Y. Hayashi, Y. Kojima, A. Nakane, K. Tozawa, K. Kohri, Activation of NF-kappa B associated with germ cell apoptosis in testes of experimentally induced cryptorchid rat model, Urology 73 (2009) 389–393.
[41] J.J. Lysiak, H.J. Bang, Q.A. Nguyen, T.T. Turner, Activation of the nuclear factor kappa B pathway following ischemia–reperfusion of the murine testis, J. Androl. 26 (2005) 129–135.
[42] V. Pentikainen, L. Suomalainen, K. Erkkila, E. Martelin, M. Parvinen, M.O. Pentikäinen, L. Dunkel, Nuclear factor-kappa B activation in human testicular apoptosis, Am. J. Pathol. 160 (2002) 205–218.
[43] R.J. Rasoulpour, K. Boekelheide, NF-kappa B is activated in the rat testis following exposure to mono-(2-ethylhexyl) phthalate, Biol. Reprod. 72 (2005) 479–486.
[44] R.J. Rasoulpour, K. Boekelheide, NF-kappa B activation elicited by ionizing radiation is proapoptotic in testis, Biol. Reprod. 76 (2007) 279–285.
[45] M.S. Hayden, S. Ghosh, Signaling to NF-κB, Genes Dev. 18 (2004) 2195–2224.
[46] D. Frank, H.W. William, Stage-specific nuclear expression of NF-kB in mammalian testis, Mol. Endocrinol. 12 (1998) 1696–1707.